

1 **Third dose COVID-19 mRNA vaccine enhances IgG4 isotype switching and recognition**
2 **of Omicron subvariants by memory B cells after mRNA but not adenovirus priming**

3

4 **AUTHORS**

5 Gemma E. Hartley¹, Holly A. Fryer¹, Paul A. Gill¹, Irene Boo², Scott J. Bornheimer³, P. Mark
6 Hogarth^{1,4,5}, Heidi E. Drummer^{2,6,7}, Robyn E. O’Hehir^{1,8}, Emily S.J. Edwards¹ and Menno C.
7 van Zelm^{1,8*}

8

9 ¹ Allergy and Clinical Immunology Laboratory, Department of Immunology, Central Clinical
10 School, Monash University, Melbourne, VIC, Australia;

11 ² Viral Entry and Vaccines Group, Burnet Institute, Melbourne, VIC, Australia;

12 ³ BD Biosciences, San Jose, CA, USA;

13 ⁴ Immune Therapies Group, Burnet Institute, Melbourne, VIC, Australia;

14 ⁵ Department of Pathology, The University of Melbourne, Parkville, VIC, Australia;

15 ⁶ Department of Microbiology and Immunology, Peter Doherty Institute for Infection and
16 Immunity, University of Melbourne, Melbourne, VIC, Australia;

17 ⁷ Department of Microbiology, Monash University, Clayton, VIC, Australia;

18 ⁸ Allergy, Asthma and Clinical Immunology Service, Alfred Hospital, Melbourne, VIC,
19 Australia

20

21 *Corresponding author: Menno C. van Zelm, Department of Immunology, Central Clinical

22 School, Monash University, 89 Commercial Road, Melbourne, VIC 3004,

23 Australia. Email: menno.vanzelm@monash.edu

24 **ABSTRACT**

25 **Background:** Booster vaccinations are recommended to improve protection against severe
26 disease from SARS-CoV-2 infection. With primary vaccinations involving various adenoviral
27 vector and mRNA-based formulations, it remains unclear if these differentially affect the
28 immune response to booster doses. We here examined the effects of homologous
29 (mRNA/mRNA) and heterologous (adenoviral vector/mRNA) vaccination on antibody and
30 memory B cell (Bmem) responses against ancestral and Omicron subvariants.

31 **Methods:** Healthy adults who received primary BNT162b2 (mRNA) (n=18) or ChAdOx1
32 (vector) (n=25) vaccination were sampled 1-month and 6-months after their 2nd and 3rd dose
33 (homologous or heterologous) vaccination. Recombinant spike receptor-binding domain
34 (RBD) proteins from ancestral, Omicron BA.2 and BA.5 variants were produced for ELISA-
35 based serology, and tetramerized for immunophenotyping of RBD-specific Bmem.

36 **Results:** Dose 3 boosters significantly increased ancestral RBD-specific plasma IgG and
37 Bmem in both cohorts. Up to 80% of ancestral RBD-specific Bmem expressed IgG1⁺. IgG4⁺
38 Bmem were detectable after primary mRNA vaccination, and expanded significantly to 5-
39 20% after dose 3, whereas heterologous boosting did not elicit IgG4⁺ Bmem. Recognition of
40 Omicron BA.2 and BA.5 by ancestral RBD-specific plasma IgG increased from 20% to 60%
41 after the 3rd dose in both cohorts. Reactivity of ancestral RBD-specific Bmem to Omicron
42 BA.2 and BA.5 increased following a homologous booster from 40% to 60%, but not after a
43 heterologous booster.

44 **Conclusion:** A 3rd mRNA dose generates similarly robust serological and Bmem responses
45 in homologous and heterologous vaccination groups. The expansion of IgG4⁺ Bmem after
46 mRNA priming might result from the unique vaccine formulation or dosing schedule
47 affecting the Bmem response duration and antibody maturation.

48 INTRODUCTION

49 Severe acute respiratory coronavirus-2 (SARS-CoV-2) causing the coronavirus disease-2019
50 (COVID-19) pandemic has resulted in over 750 million infections and over 6.9 million deaths
51 (1). To combat the worldwide pandemic, the scientific community rapidly developed new
52 vaccination technologies to reduce the burden of infections. Novel mRNA (BNT162b2 and
53 mRNA-1273) and adenoviral vector (ChAdOx1 and Ad26.COV2.S) formulations were used
54 in primary vaccination schedules across the globe (2-6) with high protection against severe
55 disease (85-100%) (6-8). These vaccines generate responses to the SARS-CoV-2 spike
56 protein, inducing antibodies directed to the receptor binding domain (RBD) that can prevent
57 viral entry into host cells (2-6). Due to the nature of these vaccines to induce host cell
58 expression of viral spike proteins, these elicit both high antibody titers and memory B cell
59 (Bmem) numbers, as well as CD4⁺ and CD8⁺ T cell responses to protect against viral
60 infection (2, 4).

61 In Australia, the initial primary vaccinations in 2021 were performed with two doses of
62 BNT162b2 or ChAdOx1 with either a 3-4 week interval (2) or a 12-week interval (5, 9),
63 respectively. Following the link between ChAdOx1 and vaccine-induced thrombocytopenia
64 and thrombosis (10, 11), from April 2021 mRNA vaccinations (BNT162b2 or mRNA1273)
65 were preferentially used in primary schedules and subsequent booster vaccinations. Due to
66 border closures and COVID-19 restrictions, SARS-CoV-2 infection rates were low across
67 Australia until late 2021 when the Delta subvariant caused a spike in infections. However,
68 infection rates overall remained low, and the adult population had the opportunity to obtain 3
69 vaccine doses before more widespread infections with the Omicron variant (12-14).

70 Primary BNT162b2 vaccination generates robust antibody and Bmem responses with a
71 predominant IgG1⁺ Bmem response (14, 15). The second dose also increased the reactivity of
72 antibodies and Bmem to SARS-CoV-2 variants (14, 15). While the antibody response

73 contracts after 1 month, Bmem numbers, their capacity to recognize viral variants, and their
74 levels of somatic hypermutation (SHM) continue to increase up to 6-months post-vaccination
75 (16-18). This suggests that there might be ongoing Bmem maturation due to continual
76 germinal center (GC) activity (16, 17) which could be supported by spike-specific T follicular
77 helper cells (Tfh), which remain stably present in GCs up to 6-months post-vaccination (19).

78 The immune response to primary adenoviral vector vaccination has not been as
79 extensively studied. While it elicits significantly lower antibody levels than BNT162b2
80 vaccination (12, 20), it generates similar numbers of ancestral (Wuhan-Hu-1; WH1) RBD-
81 specific Bmem numbers (12), which are also durable up to 6-months post-vaccination (20,
82 21). Still, to date there is little evidence to suggest that primary adenoviral vector vaccination
83 induces continual Bmem maturation or GC activity.

84 Third dose booster vaccinations were successful in boosting protection against severe
85 disease from SARS-CoV-2 variants including Omicron (22-24). In addition to higher serum
86 IgG (22, 25, 26), a third dose mRNA booster was shown to increase the proportion of IgG-
87 switched spike-specific Bmem (22, 26). Interestingly, this third dose booster also induced
88 serum IgG4 and an expansion of Bmem expressing IgG4 (26). IgG4⁺ Bmem are mostly
89 CD27⁺ and contain high levels of SHM, suggestive of an origin from secondary responses
90 (27). As IgG4 responses are uncommon after other booster vaccinations (eg. Influenza) (28),
91 it remains unclear whether this phenomenon is related to the antigen or to the vaccine
92 formulation. Here, we addressed this by detailed evaluation of the antibody and Bmem
93 response in individuals who received a homologous (primary mRNA with mRNA boost) or
94 heterologous (primary adenoviral vector with mRNA boost) COVID-19 vaccination
95 schedule.

96 **METHODS**

97 **Participants**

98 Healthy individuals without hematological or immunological disease, who had decided to
99 take the COVID-19 vaccine were enrolled in a low-risk research study to examine their
100 immune response to vaccination. Following informed consent, basic demographics (age and
101 sex) were collected, as well as blood samples before and after each of three vaccinations
102 between March 2021 and July 2022. The volunteers received either homologous (primary 2-
103 dose BNT162b2 followed by BNT162b2 third dose, n = 18) or heterologous (primary 2-dose
104 ChAdOx1 nCoV-19 followed by BNT162b2 third dose, n = 25) vaccinations. Of the 43 third
105 dose boosters, one was mRNA-1273 and the other 42 were BNT162b2 (**Supplementary**
106 **tables 1 and 2**). The cohorts were established previously, and responses were reported pre-
107 vaccination, 3-4 weeks after dose 1 and 1 month after dose 2 (*12, 14*). For this study, samples
108 were evaluated that were obtained 1 and 6 months after doses 2 and 3. This study was
109 conducted according to the principles of the Declaration of Helsinki and approved by local
110 human research ethics committees (Alfred Health ethics no. 32-21/Monash University project
111 no. 72794).

112

113 **Sample processing**

114 Blood samples were processed as described previously (*28-30*). Briefly, 200 μ l was used for
115 whole blood cell counts (Cell-Dyn analyzer; Abbott Core Laboratory, Abbott Park, IL) and
116 Trucount analysis (see flow cytometry section). The remainder of the sample was used to
117 separate and store plasma (-80°C), and to isolate live peripheral blood mononuclear cells
118 (PBMC) following Ficoll-paque density gradient centrifugation and cryopreservation in
119 liquid nitrogen for later analysis of RBD-specific B cells.

120

121 **Protein production and tetramerization**

122 Recombinant spike RBD and nucleoprotein (NCP) proteins of the SARS-CoV-2 ancestral,
123 Delta and Omicron BA.2 and BA.5 subvariant RBDs were produced with the N-terminal Fel
124 d 1 leader sequence and C-terminal biotin ligase (BirA) AviTag and 6-His affinity tags, as
125 described previously (14, 30). The RBD from the SARS-CoV-2 variants contained the
126 following mutations: B.1.617.2 (Delta) L452R, T478K; B.1.1.529 (Omicron BA.2): G339D,
127 S371F, S373P, S375F, S376A, D405N, R408S, K417N, N440K, S477N, T478K, E484A,
128 Q493K, Q498R, N501Y, Y505H; B.1.1.529 (Omicron BA.5): BA.2 mutations with
129 additional L452R, F486V and reversion of Q498. The DNA constructs were cloned into a
130 pCR3 plasmid and produced and purified as described previously (14, 30). DNA was
131 transfected into 293F cells using the Expi293 Expression system (Thermo Fisher Scientific,
132 Waltham, MA). Following 5-day cultures at 37°C (ancestral and Delta) or 34°C (Omicron
133 subvariants), harvested supernatants were purified using a Talon NTA-cobalt affinity column
134 (Takara Bio, Kusatsu, Shiga, Japan) with elution in 200 mM Imidazole. Purified proteins
135 were then dialyzed into 10 mM Tris and biotinylated (14, 30). Biotinylated proteins were
136 subsequently dialyzed against 10 mM Tris for 36 hours at 4°C with 3 or more exchanges, and
137 subsequently stored at -80°C prior to use. Soluble biotinylated RBD proteins were
138 tetramerized with unique fluorochrome-conjugated streptavidins at a protein:streptavidin
139 molar ratio of 4:1 to form: [RBD WH1]₄-BUV395, [RBD WH1]₄-BUV737, [RBD BA.2]₄-
140 BV480 and [RBD BA.5]₄-BV650.

141

142 **Measurement of SARS-CoV-2 neutralizing antibodies in plasma**

143 Measurement of neutralizing antibodies was performed using SARS-CoV-2 retroviral
144 pseudotyped particles and a 293T-ACE2 cell line, as described previously (14, 30). Briefly,
145 plasma was heat inactivated at 56°C for 45 minutes and serially diluted in DMF10. Diluted

146 samples were then mixed with an equal volume of SARS-CoV-2 (Wuhan-1 Ancestral, Delta,
147 BA.2 and BA.4/5 spike) retroviral pseudotyped virus and incubated for 1 hour at 37°C.
148 Virus-plasma mixtures were added to 293T-ACE2 monolayers seeded the day prior at 10,000
149 cells/well, incubated for 2 hours at 37°C, before addition of an equal volume of DMF10 and
150 incubated for 3 days. After incubation, tissue culture fluid was removed, and monolayers
151 were washed once with PBS and lysed with cell culture lysis reagent (Promega, Madison,
152 WI) and luciferase measured using luciferase substrate (Promega) in a Clariostar plate reader
153 (BMG LabTechnologies, Offenburg, Germany). The percentage entry was calculated as
154 described previously (14, 30), and plotted against reciprocal plasma dilution GraphPad Prism
155 9 Software (GraphPad Software, La Jolla, CA) and curves fitted with a one-site specific
156 binding Hill plot. The reciprocal dilution of plasma required to prevent 50% virus entry was
157 calculated from the non-linear regression line (ID50). The lowest amount of neutralizing
158 antibody detectable is a titer of 20. All samples that did not reach 50% neutralization were
159 assigned an arbitrary value of 10.

160

161 **ELISA**

162 For quantification of total IgG against NCP and ancestral RBD and NCP, EIA/RIA plates
163 (Costar, St Louis, MO) were coated with 2µg/ml recombinant SARS-CoV-2 ancestral RBD
164 or NCP overnight at 4°C. Wells were blocked with 3% BSA in PBS and subsequently
165 incubated with plasma samples. Plasma was diluted 1:300 for quantification of ancestral
166 RBD- and NCP-specific antibodies post-dose 2, 6-months post-dose 2, post-dose 3 and 6-
167 months post-dose 3. Plasma was titrated from 1:30 to 1:10,000 for quantification of ancestral
168 and variant RBD-specific antibodies post-dose 2 and 3. Antigen-specific IgG was detected
169 using rabbit anti-human IgG HRP (Dako, Glostrup, Denmark). ELISA plates were developed
170 using TMB solution (Life Technologies, Carlsbad, CA) and the reaction was stopped with 1

171 M HCl. Absorbance (OD450nm) was measured using a Multiskan Microplate
172 Spectrophotometer (Thermo Fisher Scientific). Serially diluted recombinant human IgG (in-
173 house made human Rituximab) was used for quantification of specific IgG in separate wells
174 on the same plate. Area under the curve (AUC) was calculated for each titration curve using
175 GraphPad Prism software. Relative recognition of the RBD variants was calculated as a
176 percentage of the AUC for that variant relative to the AUC for ancestral RBD.

177 For quantification of ancestral RBD-specific IgG1 and IgG4, EIA/RIA plates (Costar)
178 were coated with 2 or 1 µg/ml recombinant SARS-CoV-2 ancestral RBD overnight at 4°C for
179 IgG1 and IgG4 ELISAs respectively. Wells were blocked with 5% skim milk powder (SMP)
180 in PBS and subsequently incubated with plasma samples. Plasma was diluted from 1:100 to
181 1:2000 for quantification of ancestral RBD-specific IgG1 and IgG4 antibodies post-dose 2, 6-
182 months post-dose 2, post-dose 3 and 6-months post-dose 3 using mouse anti-human IgG1
183 biotin (Thermo Fisher Scientific) and mouse anti-human IgG4 biotin (Sigma-Aldrich, St
184 Louis, MO), respectively. Finally, high sensitivity streptavidin HRP (Thermo Fisher
185 Scientific) was added, and ELISA plates were developed using TMB solution (Life
186 Technologies, Carlsbad, CA) and the reaction was stopped with 1 M HCl. Absorbance
187 (OD450nm) was measured using a Multiskan Microplate Spectrophotometer (Thermo Fisher
188 Scientific). Serially diluted recombinant human IgG1 or human IgG4 (BioRad, Hercules, CA)
189 with unrelated specificities were used for quantification in separate wells on the same plate.

190

191 **Flow cytometry**

192 Absolute numbers of leukocyte subsets were determined as previously described (29, 30).
193 Briefly, 50 µl of whole blood was added to a Trucount tube (BD Biosciences) together with
194 20 µl of antibody cocktail containing antibodies to CD3, CD4, CD8, CD16, CD19, CD56 and
195 CD45 from the 6-color TBNK reagent kit (BD Biosciences) (**Supplementary Tables 4 and**

196 5) and incubated for 15 minutes at room temperature in the dark. Subsequently, samples were
197 incubated for a further 15 minutes at room temperature with 500 µl of 1X BD Lysis solution
198 (BD Biosciences) to lyse red blood cells. The tube was then stored in the dark at 4°C for up to
199 2 hours prior to acquisition on a LSRII or FACSLyric analyzer (BD Biosciences).

200 For the detection of antigen-specific Bmem, cryopreserved PBMC were thawed and
201 stained as previously described (12, 14, 30). Briefly, 10-15 million PBMC were incubated
202 with fixable viability stain 700 (BD Biosciences), antibodies against CD3, CD19, CD21,
203 CD27, CD38, CD71, IgA, IgD, IgG1, IgG2, IgG3, IgG4, (**Supplementary Tables 4 and 5**)
204 and 5 µg/ml each of [RBD WH1]₄-BUV395, [RBD WH1]₄-BUV737, and [RBD BA.2]₄-
205 BV480 and [RBD BA.5]₄-BV650 for 15 minutes at room temperature in a total volume of
206 250 µl FACS buffer (0.1% sodium azide, 0.2% BSA in PBS). In addition, 5 million PBMC
207 were similarly incubated with fixable viability stain 700 (BD Biosciences), antibodies against
208 CD3, CD19, CD27 and IgD, and BUV395-, BUV737-, BV480- and BV650-conjugated
209 streptavidin controls (**Supplementary Tables 4 and 5**). Following staining, cells were
210 washed with FACS buffer, fixed with 2% paraformaldehyde for 20 minutes at room
211 temperature and washed once more. Following filtration through a 70 µM filter, cells were
212 acquired on a 5-laser LSRFortessa X-20 (BD Biosciences). Flow cytometer set-up and
213 calibration was performed using standardized EuroFlow SOPs, as previously described
214 (**Supplementary Tables 6 and 7**) (31).

215

216 **Data analysis and statistics**

217 All flow cytometry data were analyzed with FlowJo v10 software (BD Biosciences).
218 Statistical analysis was performed with GraphPad Prism 9 Software (GraphPad Software).
219 Matched pairs were analyzed with the non-parametric Wilcoxon matched pairs signed rank
220 test with Bonferroni correction for multiple comparisons. Comparisons between 3 or more

221 groups were performed using the Friedman's test (paired) or Kruskal-Wallis (unpaired) with
222 Dunn multiple comparisons test. For all tests, $p < 0.05$ was considered significant.

223 **RESULTS**

224 **Third dose booster increases ancestral RBD-specific Bmem irrespective of primary** 225 **vaccination formulation**

226 Blood samples were collected at 1 and 6 months after both dose 2 (D2 and 6mD2,
227 respectively) and dose 3 (D3 and 6mD3, respectively) from 18 individuals who received a
228 homologous vaccination schedule (3x mRNA) and 25 individuals who received heterologous
229 vaccination (2x ChAdOx1, 1x mRNA) (**Figure 1A, Supplementary Tables 1, 2, 3**). There
230 were no significant differences in sampling times between the two cohorts apart from 6-
231 months post-dose 2: 185 (homologous) vs 178 days (heterologous) ($p < 0.0001$)
232 (**Supplementary Table 3**). The cohorts did not differ in age, but the homologous group
233 trended to include fewer females (56%) than the heterologous group (80%; $p = 0.09$)
234 (**Supplementary Tables 1 and 2**).

235 The vaccine-specific antibody and Bmem responses were evaluated using
236 recombinantly-produced RBD proteins of ancestral and Omicron BA.2 and BA.5, whereas
237 SARS-CoV-2 nucleocapsid protein (NCP)-specific plasma IgG and was evaluated to confirm
238 self-reported breakthrough infections (BTI) (*12, 14, 30*). As previously reported (*12, 14*), our
239 BNT162b2 cohort had 8-10-fold higher ancestral RBD-specific plasma IgG and neutralizing
240 antibodies (NAb) than the ChAdOx1 cohort at 1-month post-dose 2 (**Figure 1B, C**). The third
241 dose mRNA booster elicited similar RBD-specific IgG and NAb responses in both cohorts,
242 with levels comparable to those of the mRNA cohort after dose 2 (**Figure 1B, C**).
243 Importantly, all donors generated detectable NAb after dose 3, even those four that did not
244 reach neutralizing capacity after 2 doses of ChAdOx1 (**Figure 1C**).

245 Ancestral RBD-specific Bmem were evaluated within CD19⁺ B cells after exclusion of
246 CD27⁺IgD⁺ naive B cells (**Supplementary Figure 1**) through double discrimination, i.e.
247 positivity for both [RBD WH1]₄-BUV395 and [RBD WH1]₄-BUV737 (**Figure 1D**). The
248 primary BNT162b2 and ChAdOx1 vaccinated cohorts had similar ancestral RBD-specific
249 Bmem numbers after dose 2 (**Figure 1E**) (12). The third mRNA dose significantly increased
250 ancestral RBD-specific Bmem numbers in both cohorts irrespective of the primary schedule
251 (**Figure 1E**).

252

253 **Durability of ancestral RBD-specific Bmem up to 6 months after 2 and 3 vaccine doses**

254 To evaluate the durability of the response, the vaccine-induced antibody levels and Bmem
255 numbers were quantified and compared between 1- and 6-months post-dose 2 and 3. Multiple
256 participants self-reported SARS-CoV-2 BTI, and these were confirmed with NCP-specific
257 plasma IgG (12, 14) (**Supplementary Tables 1 and 2**) (**Figure 2 A, E**). These samples are
258 marked (green triangles) to visualize a potential confounding effect (**Figure 2A-H**). In line
259 with previous observations, the plasma IgG and NAb levels contracted between 1 and 6
260 months after both dose 2 and dose 3 (**Figure 2B,C,F,G**). Within the complete cohorts, the
261 contractions were not significant after dose 3. This was due to a confounding effect of BTIs:
262 Following stratification, this decline was significant for the groups without BTI (**Figure 2B,**
263 **F**).

264 Double dose primary BNT162b2 vaccination generated a population of ancestral RBD-
265 specific Bmem that trended to increase in number at 6-months post-dose 2 (prior to the third
266 dose), however, this was not seen in the heterologous cohort (**Figure 2D, H**). The third dose
267 significantly boosted ancestral RBD-specific Bmem numbers in both cohorts with
268 heterologous vaccination generating a wider range of Bmem numbers (**Figure 2D, H**).
269 Individuals who had BTIs between 1- and 6-months post-dose 3 trended to have higher

270 numbers of ancestral RBD-specific Bmem at 6-months post-dose 3. No significant decline of
271 ancestral RBD-specific Bmem numbers was observed in SARS-CoV-2 naive individuals at 6-
272 months post-dose 3 in either cohort (**Figure 2D, H**). In summary, irrespective of primary
273 vaccination, the antibody responses contract between 1 and 6 months after doses 2 and 3,
274 whereas the ancestral RBD-specific Bmem numbers remain more stable.

275 **Transient expansion of recently activated ancestral RBD-specific Bmem at 1 month** 276 **after mRNA vaccination**

277 To evaluate the maturation status of ancestral RBD-specific Bmem, these were further
278 evaluated for surface marker expression (**Figure 3A**). CD71 is expressed on recently
279 activated cells to provide uptake of iron for proliferation (32, 33) and is typically
280 downregulated within 14 days (30, 34). Both cohorts at all timepoints had only minor
281 fractions and numbers of vaccine induced RBD-specific Bmem (median <3%) expressing
282 CD71, indicative of quiescent populations (**Figure 3B, Supplementary Figure 2A**). The
283 exceptions were 3 samples in the heterologous cohort that were obtained within 15 days of
284 BTI (participants no. 20, 34 and 42) (**Figure 3B, Supplementary Table 2**). Low expression
285 of CD21 on Bmem is another marker of recent activation (35). While the majority of RBD-
286 specific Bmem at 1 month after doses 2 and 3 were CD21⁺, frequencies of CD21^{lo} cells
287 significantly increased at 1 month and then significantly declined at 6-months after each dose
288 (**Figure 3C, Supplementary Figure 2B**). Finally, expression of CD27 was evaluated within
289 RBD-specific IgG⁺ Bmem as a marker for more mature IgG⁺ Bmem (36, 37). The majority of
290 RBD-specific IgG⁺ Bmem were CD27⁺ 1 month after dose 2 with was no significant
291 difference in frequency between cohorts at this timepoint ($p = 0.23$). However, frequencies
292 significantly increased 6 months after dose 2 and 3 mRNA vaccination, but not 6 months
293 after dose 2 adenoviral vector vaccination (**Figure 3D**). Together this phenotypic evaluation
294 demonstrates that at 1 month after each vaccine, the RBD-specific Bmem populations do not

295 display signs of recent proliferation, similar to the total Bmem compartment (**Supplementary**
296 **Figure 3**). Still, the RBD-specific Bmem at 1-month post-dose 2 and dose 3 contain large
297 fractions of recently activated cells that further mature by 6 months, thereby gaining CD21
298 and CD27 expression. These signs of further maturation between 1 and 6 months are
299 particularly notable following mRNA vaccination.

300

301 **Expansion of IgG4⁺ Bmem after homologous boost is absent from heterologous boost**

302 To investigate whether the previously observed IgG4 response (26, 38) also occurred in our
303 cohorts, we evaluated the plasma IgG1 and IgG4 subclass contributions to the homologous or
304 heterologous third dose booster responses. Both cohorts generated high levels of ancestral
305 RBD-specific plasma IgG1 after the third dose, and these recapitulated the dynamics of the
306 total ancestral RBD-specific IgG (**Figure 4A**). Ancestral RBD-specific plasma IgG4 was
307 detectable at low level in the mRNA primed cohort, and these levels were boosted after the
308 third dose (**Figure 4B**). In contrast, the adenoviral vector primed cohort showed very little
309 IgG4 prior to and after the third dose boost (**Figure 4B**). Thus, priming with an mRNA or
310 adenoviral vector vaccine has differential effects on the capacity of recipients to form IgG4
311 responses.

312 IgG4⁺ Bmem are presumed to be formed after ongoing GC responses or after renewed
313 encounters with the same antigen (27). Therefore, we here evaluated vaccine-elicited
314 formation of IgG4⁺ Bmem in the two cohorts before and after the third dose booster. Through
315 our extensive immunophenotyping including Ig isotypes and IgG subclasses, we previously
316 found expansions of IgG1⁺, but not IgG4⁺ Bmem after 2 doses of BNT162b2 or ChAdOx1 in
317 COVID-19 naïve individuals (12, 14). With the same approach (**Supplementary Figure 1A,**
318 **B**), we here found that in both cohorts the ancestral RBD-specific IgG1⁺ Bmem population
319 remained stable at 6-months post-dose 2 and was further expanded after dose 3 (**Figure 4C-**

320 **E, Supplementary Figures 1C, 4 and 5).** The IgM⁺ Bmem and IgA⁺ Bmem populations
321 were not affected (**Fig 4C-E, Supplementary Figures 4-6**). At 6-months post-dose 3, the
322 IgG1 compartment encompassed approximately 80-90% of the ancestral RBD-specific
323 Bmem compartment (**Figure 4C, D**). This enrichment was not apparent in the total Bmem
324 compartment, in which only about 20% expressed IgG1 (**Supplementary Figure 7**).
325 Importantly, the BNT162b2-primed cohort showed a significant enlargement of the ancestral
326 RBD-specific IgG4⁺ Bmem compartment at 6-months post-dose 2 (**Figure 4C, E,**
327 **Supplementary Figure 1D**). This population was further expanded at 1- and 6-months post-
328 dose 3. In contrast, the ChAdOx1-primed cohort had very few ancestral RBD-specific IgG4⁺
329 Bmem at each timepoint (**Figure 4D, E**), except for one individual who had a BTI prior to
330 the 6-months post-dose 3 sample. Thus, the expansion of plasma IgG4 and IgG4⁺ Bmem after
331 a third dose booster is restricted to the mRNA-primed cohort, suggesting that either the
332 primary vaccination formulation or the unique primary dosing schedule (3-week interval)
333 underlies this.

334

335 **An mRNA booster enhances recognition of Omicron subvariants by Bmem irrespective** 336 **of primary vaccination**

337 To examine the effect of mRNA booster vaccination on recognition of SARS-CoV-2
338 variants, we evaluated the capacity of plasma antibodies and ancestral-RBD-specific Bmem
339 to recognize Delta (B.1.617.2) and Omicron (B.1.1.529) BA.2 and BA.5 variant RBD
340 proteins. NAb levels to all three variants were significantly higher at 1-month post-dose 3
341 than at 1-month post-dose 2 for both cohorts (**Figure 5A, B**). Importantly, after dose 3,
342 plasma from all donors had the capacity to neutralize all variants, whereas only all
343 individuals generated NAbs to Delta after 2 doses of BNT162b2(**Figure 5A, B**). Plasma
344 RBD-binding serology was performed to evaluate the relative capacity of ancestral RBD-

345 specific IgG to bind each variant. In line with previous findings, the capacity of ancestral
346 RBD-specific plasma IgG to bind Delta RBD was almost 100% (**Figure 5C, D**). In contrast,
347 the median recognition of BA.2 and BA.5 was <30% after 2 vaccine doses, irrespective of
348 formulation, and these increased significantly after the third dose mRNA booster to 50-60%
349 (**Figure 5C, D**).

350 In addition, we used fluorescent tetramers of Omicron BA.2 and BA.5 RBDs to evaluate
351 the capacity of ancestral RBD-specific Bmem to bind either or both subvariants (**Figure 5E**).
352 Around 30-40% of ancestral RBD-specific Bmem bound BA.2 at 1-month post-dose 2 in
353 both cohorts, and this recognition significantly increased to 60% at 6-months post-dose 2
354 (**Figure 5F**). BA.2 recognition 1-month post-dose 3 was about 50% and this increased in the
355 homologous cohort to 60% at 6-months post-dose 3, whereas no change was observed at 6-
356 months post-dose 3 in the heterologous cohort (**Figure 5F**). Recognition of BA.5 showed
357 similar patterns as BA.2 in the homologous cohort with significant increases from 30% to
358 50% at 1-month and 6-months post-dose 2, as well as from 40% to 60% at 1- and 6-months
359 post-dose 3 (**Figure 5G**). In contrast, no significant changes were found for recognition of
360 BA.5 in the heterologous group with median recognition in the range of 40-50% (**Figure**
361 **5G**). Variant-binding ancestral RBD-specific Bmem also showed a similar phenotype (ie.
362 predominantly IgG1⁺ with IgG enrichment in the homologous group) to total ancestral RBD-
363 specific Bmem in each respective vaccination cohort (**Supplementary Figure 8**).

364 In summary, we confirm previous findings that a third dose mRNA booster significantly
365 expands ancestral RBD-specific plasma IgG and Bmem levels, irrespective of the primary
366 vaccination schedule. Importantly, we expanded on previous observations that the formation
367 of plasma IgG4 and IgG4⁺ Bmem is restricted to mRNA-primed individuals, and not present
368 in adenoviral vector vaccine-primed individuals who are COVID-19 naive. While Bmem at
369 1-month post-vaccination appear to be quiescent, these do show signs of recent activation

370 which are absent at 6-months post-vaccination. This ongoing maturation is associated with
371 increased recognition of Omicron variants and is especially apparent after mRNA
372 vaccination.

373 **DISCUSSION**

374 We have shown that both homologous and heterologous COVID-19 booster vaccinations
375 significantly increase ancestral RBD-specific plasma IgG and Bmem. An mRNA third dose
376 induces a population of recently activated Bmem, but these contract at 6-months post-dose 3.
377 The ancestral RBD-specific Bmem population seemed to further mature with an increase in
378 the proportion of IgG⁺ Bmem that expressed CD27 at 6-months post-dose 3. Only after
379 mRNA priming, a population of IgG4⁺ RBD-specific Bmem was apparent that expanded
380 after the homologous third dose boost with increased recognition of Omicron BA.2 and BA.5
381 subvariants.

382 A third COVID-19 vaccine dose was recommended in late 2021 to all vaccinees after
383 evidence suggested that antibody levels declined beyond 6-months post-primary vaccination
384 and the risk of BTI increased (39-42). We confirm previously reported findings that a third
385 dose (either homologous or heterologous) significantly boosts RBD-specific IgG and NAb
386 levels regardless of primary vaccination formulation (22, 43-45). Ancestral RBD-specific
387 Bmem numbers are also significantly increased following the third dose. We have previously
388 shown that primary vaccination with either BNT162b2 or ChAdOx1 generated similar
389 numbers of ancestral RBD-specific Bmem (12). We have expanded on this by demonstrating
390 that in contrast to ancestral RBD-specific plasma IgG and NAb levels, ancestral RBD-
391 specific Bmem numbers did not significantly decline at 6-months post-dose 3, in line with
392 other studies (16, 22, 46, 47).

393 Previous studies have used increased CD71 expression and reduced CD21 expression as
394 markers of recently activated Bmem (34, 35). The observed dynamics of CD71 expression in
395 this study are in line with our previous findings following primary COVID-19 vaccination
396 and others post-influenza vaccination, with CD71⁺ Bmem contracting beyond 7 days post-
397 antigen exposure (12, 14, 34). Heterologous vaccination induces a significant expansion of

398 CD21^{lo} ancestral RBD-specific Bmem that is still apparent 4 weeks after the third dose (30-
399 40% of the compartment). In previous studies, we have shown that less than 30% of ancestral
400 RBD-specific Bmem were CD21^{lo} 4 weeks after primary (double-dose) COVID-19
401 vaccination (12, 14). However, others have shown that this CD21^{lo} activated memory
402 population can make up to 40-50% of the antigen-specific Bmem population 4 weeks after
403 either influenza or COVID-19 vaccination, or SARS-CoV-2 infection, and does not contract
404 to below 25% until after 90 days following vaccination (35, 48). Therefore, although the
405 frequencies of CD21^{lo} Bmem observed following a third dose are higher than we have
406 observed following primary COVID-19 vaccination, these levels are consistent with previous
407 studies from other groups (34, 35).

408 Following the third dose booster, the frequencies of IgG⁺ Bmem that expressed CD27
409 initially declined at 1-month, followed by a significant increase at 6 months. Thus, the initial
410 vaccine elicited Bmem population continued to mature for several months after mRNA
411 booster vaccination. As CD27⁺IgG⁺ Bmem have higher levels of SHM and an increased
412 replication history than CD27⁻IgG⁺ Bmem, these likely originate from ongoing or renewed
413 GC reactions (36, 37). The CD21^{lo} Bmem compartment can comprise of cells either primed
414 for plasma cell differentiation (CD21^{lo}CD27⁺) (49) or from extrafollicular responses
415 (CD21^{lo}CD27⁻) (48, 50), and are thus unlikely to contribute to the long-term stability of the
416 Bmem compartment. Hence, we infer that the increase in the proportion of CD27⁺IgG⁺
417 Bmem is indicative of continual GC activity and maturation beyond 1-month post-mRNA
418 booster vaccination. Continual GC responses can generate a high affinity resting Bmem pool,
419 which is important to maintain durable protection while recently activated Bmem numbers
420 continue to decrease (51, 52).

421 Primary COVID-19 vaccination generated a predominant IgG1⁺ population of ancestral
422 RBD-specific Bmem in both cohorts, which was further expanded after a third dose boost.

423 Importantly, the expansion of IgG1⁺ Bmem was not at the expense of IgM⁺ Bmem, which
424 remained present in similar numbers. IgG1⁺ Bmem can provide protection against BTI by
425 secreting IgG1 antibodies upon re-exposure. IgG1 antibodies are potent neutralizers and are
426 effective at activating the classical complement pathway and engaging Fc-mediated responses
427 such as antibody-dependent cellular cytotoxicity and hence are important in the clearance of
428 viral infections (53, 54). Thus, a predominant IgG1 response following COVID-19
429 vaccination is suitable for neutralization of this pathogen.

430 We here found that the significant expansion of IgG4⁺ Bmem after the third dose boost
431 (26) was only apparent in the mRNA-primed cohort and not in the adenoviral vector-primed
432 group. Thus, it raises the question as to the mechanisms that drive the formation of IgG4-
433 secreting plasma cells and IgG4⁺ Bmem. Other vaccinations have generated the production of
434 plasma IgG4 such as VAX003 (HIV), EBA-175 (Malaria) and acellular pertussis
435 vaccinations (55-57). It is not well understood why these vaccine formulations and schedules
436 induce IgG4 antibodies. However, it is worth noting that VAX003 has a multiple-dose
437 schedule (7 doses) in comparison to other HIV vaccine candidates that are given as a single
438 dose (55). In addition, IgG4 antibodies are also produced in response to the repeated antigen
439 exposure of allergen immunotherapy (58, 59). Given the unique capacity of IgG4 antibodies
440 to undergo Fab arm exchange, there could be a unique functional effect elicited by mRNA
441 vaccination, although it should be noted that IgG1 still predominates the response.

442 Primary BNT162b2 vaccination has a shorter window between dose 1 and dose 2 (3
443 weeks) (2) compared to ChAdOx1 (12 weeks) (5, 9). As both groups received an mRNA
444 third dose 6-months post-primary vaccination, the IgG4 expansion in the homologous group
445 is either due to the timing between dose 1 and 2 or the primary vaccination formulation.
446 Examining a cohort of individuals who received a primary mRNA vaccination with a longer
447 duration between doses 1 and 2 would confirm whether this effect is due to dosing or

448 vaccination formulation. In IgG4-related disease and Kimura disease, prominent IgG4 class
449 switching is thought to be controlled by a population of Tfh cells co-expressing CXCR5, PD-
450 1, ICOSL, IL-10, IL-4 and LAG-3 (60, 61). It would be of interest whether such a Tfh cell
451 population is specifically generated by mRNA vaccination and/or repeat vaccinations with a
452 short time interval (<1 month).

453 Whilst ancestral RBD-specific plasma IgG levels were increased at 1 month following
454 the third vaccine dose, these levels had significantly declined at 6 months in individuals
455 without a confirmed BTI. Individuals with a confirmed BTI at that timepoint showed an
456 increase in RBD-specific plasma IgG and trended to have more ancestral RBD-specific
457 Bmem. Others have also demonstrated that BTI following COVID-19 vaccination generates
458 higher antibody and Bmem responses to COVID-19 naive vaccinated individuals (47, 62,
459 63). This suggests that subsequent antigen exposures, either through vaccination or infection,
460 would continue to increase antibody and Bmem levels. However, we currently do not know if
461 there are certain levels of antibodies or B and T cell numbers required to confer protection.
462 What may be more important is not the overall boosting of the response, but enhanced
463 recognition of SARS-CoV-2 variants, that may prevent infection and/or severe disease.

464 Homologous vaccination not only induces an IgG4 expansion, but also significantly
465 increases recognition of RBD-specific Bmem to Omicron BA.2 and BA.5 up to 6-months
466 post-dose 3, whereas heterologous vaccination induces limited improvement in recognition of
467 Omicron subvariants. In contrast, both vaccination schedules showed an increase in NAb and
468 RBD-specific plasma IgG recognition of Omicron BA.2 and BA.5. This suggests that upon
469 receipt of the third dose, a number of pre-existing Bmem with a higher affinity to Omicron
470 BA.2 and BA.5 may have differentiated into antibody-secreting cells and hence increased
471 circulating antibody recognition of Omicron subvariants (64). Pre-existing Bmem can not
472 only differentiate into plasmablasts but also re-enter the GC where they undergo further SHM

473 and increase in affinity (64). mRNA primary vaccination induces continual GC activity
474 resulting in an increase in Bmem and SHM levels (16, 43, 65). Therefore, the increase in
475 SHM of ancestral RBD-specific Bmem elicited by homologous vaccination may increase the
476 affinity of the B cell receptor, allowing some variant RBD mutations impacting binding to be
477 overcome; however, further molecular studies are required to confirm this.

478 In summary, we have shown that the Bmem response elicited by a third dose booster
479 with an mRNA vaccine is differentially affected by the primary vaccination (schedule and/or
480 formulation). Both homologous and heterologous vaccine boosters significantly increased
481 ancestral RBD-specific plasma IgG, NABs, and Bmem numbers to a similar degree. Through
482 extensive immunophenotyping, we show that ancestral RBD-specific Bmem show signatures
483 of continual maturation for at least 6-months post-dose 3. However, homologous mRNA
484 vaccination alone induces an expansion of ancestral RBD-specific IgG4-switched Bmem and
485 an increased recognition of Omicron BA.2 and BA.5 by ancestral RBD-specific Bmem. It is
486 still unclear whether IgG4 is having a supportive or inhibitory role in responses to subsequent
487 boosters and what role this isotype plays in protection against disease. mRNA and adenoviral
488 vector vaccines have only been widely utilized for the first time to combat the SARS-CoV-2
489 pandemic. Their rapid production rates and high efficacies make these ideal formulations to
490 use against future pathogens. Our studies reveal how antibody and Bmem responses are
491 generated to each vaccination type as well as booster doses and reveal important differences
492 generated by each vaccine type. These vaccine technologies may be adopted to combat other
493 pathogens in the future and these data provide further crucial evidence to help public health
494 officials make informed recommendations about vaccination schedules and booster doses in
495 the future.

496

497 **ACKNOWLEDGEMENTS**

498 We thank Dr. Bruce D. Wines and Ms. Sandra Esparon (Burnet Institute) for technical
499 assistance, Ms. Shir Sun, Mr. Jack Edwards and Ms. Ebony Blight (Monash University) for
500 sample collection and preparation, and the staff of ARAFlowcore for flow cytometry support.
501 Supported by an Australian Government Research Training Program Scholarship (GEH), the
502 Australian Government Medical Research Future Fund (MRFF, Project no. 2016108; MCvZ,
503 HED and REO'H) and an unrestricted research grant from BD Biosciences.

504

505 **CONFLICTS OF INTEREST**

506 MCvZ, REO'H and PMH are inventors on a patent application related to this work. SJB is an
507 employee of and owns stock in BD. All the other authors declare no conflict of interest.

508

509 **AUTHOR CONTRIBUTIONS**

510 Designed and/or performed experiments: GEH, HAF, PAG, IB, SJB, PMH, HED, REO'H,
511 ESJE and MCvZ; Formal analysis: GEH, HAF, IB; Provided reagents: SJB; Supervised the
512 work: ESJE, REO'H and MCvZ; Wrote the manuscript: GEH and MCvZ. All authors edited
513 and approved the final version of the manuscript.

514

515 **ORCID IDs**

516 **GEH:** 0000-0002-3174-231X

517 **HAF:** 0000-0003-0779-490X

518 **PAG:** 0000-0001-8579-8493

519 **IB:** 0000-0003-0923-0972

520 **PMH:** 0000-0002-0360-7890

521 **HED:** 0000-0002-0042-6277

522 **REO'H:** 0000-0002-3489-7595

523 **ESJE:** 0000-0002-0240-4370

524 **MCvZ:** 0000-0003-4161-1919

525 REFERENCES

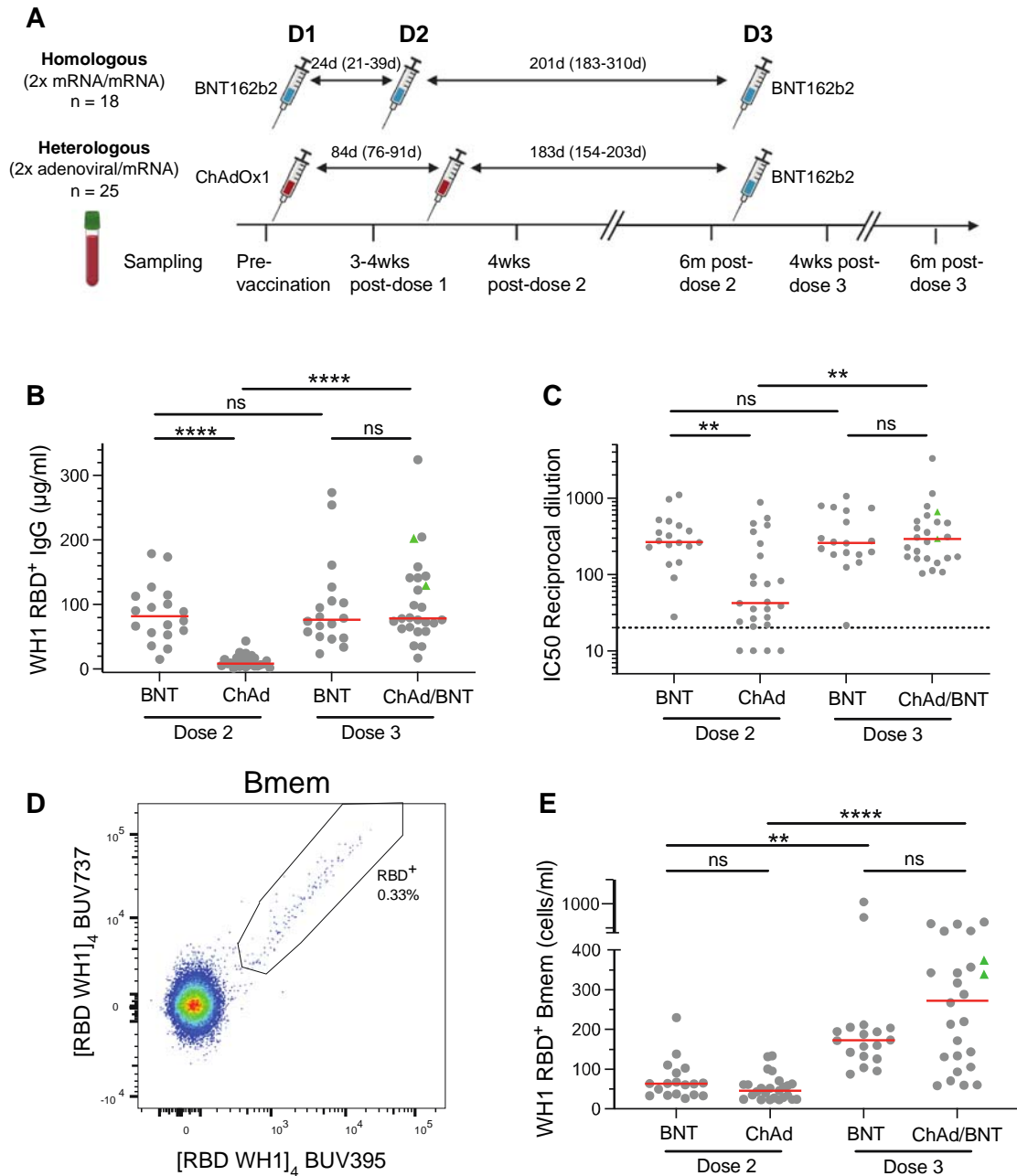
- 526 1. World Health Organisation., WHO Coronavirus (COVID-19) Dashboard,
527 <https://covid19.who.int/>, Accessed: 2/6/23
- 528 2. F. P. Polack *et al.*, Safety and Efficacy of the BNT162b2 mRNA Covid-19 Vaccine. *N*
529 *Engl J Med* **383**, 2603-2615 (2020).
- 530 3. L. R. Baden *et al.*, Efficacy and Safety of the mRNA-1273 SARS-CoV-2 Vaccine. *N*
531 *Engl J Med* **384**, 403-416 (2021).
- 532 4. P. M. Folegatti *et al.*, Safety and immunogenicity of the ChAdOx1 nCoV-19 vaccine
533 against SARS-CoV-2: a preliminary report of a phase 1/2, single-blind, randomised
534 controlled trial. *Lancet* **396**, 467-478 (2020).
- 535 5. M. Voysey *et al.*, Safety and efficacy of the ChAdOx1 nCoV-19 vaccine (AZD1222)
536 against SARS-CoV-2: an interim analysis of four randomised controlled trials in Brazil,
537 South Africa, and the UK. *Lancet* **397**, 99-111 (2021).
- 538 6. J. Sadoff *et al.*, Safety and Efficacy of Single-Dose Ad26.COV2.S Vaccine against
539 Covid-19. *N Engl J Med* **384**, 2187-2201 (2021).
- 540 7. D. S. Houry *et al.*, Neutralizing antibody levels are highly predictive of immune
541 protection from symptomatic SARS-CoV-2 infection. *Nat Med* **27**, 1205-1211 (2021).
- 542 8. H. A. Fryer, G. E. Hartley, E. S. J. Edwards, R. E. O'Hehir, M. C. van Zelm, Humoral
543 immunity and B-cell memory in response to SARS-CoV-2 infection and vaccination.
544 *Biochem Soc Trans* **50**, 1643-1658 (2022).
- 545 9. Australian Government Department of Health and Aged Care., COVID-19 vaccine
546 rollout-Full data and analysis, [https://www.health.gov.au/resources/collections/covid-19-](https://www.health.gov.au/resources/collections/covid-19-vaccine-rollout-full-data-and-analysis)
547 [vaccine-rollout-full-data-and-analysis](https://www.health.gov.au/resources/collections/covid-19-vaccine-rollout-full-data-and-analysis), Accessed: 2/6/23
- 548 10. A. Greinacher *et al.*, Thrombotic Thrombocytopenia after ChAdOx1 nCov-19
549 Vaccination. *N Engl J Med* **384**, 2092-2101 (2021).
- 550 11. S. Pavord *et al.*, Clinical Features of Vaccine-Induced Immune Thrombocytopenia and
551 Thrombosis. *N Engl J Med* **385**, 1680-1689 (2021).
- 552 12. H. A. Fryer *et al.*, COVID-19 Adenoviral Vector Vaccination Elicits a Robust Memory
553 B Cell Response with the Capacity to Recognize Omicron BA.2 and BA.5 Variants. *J*
554 *Clin Immunol*, (2023).
- 555 13. Australian Government Department of Health., Coronavirus (COVID-19) case numbers
556 and statistics, [https://www.health.gov.au/health-alerts/covid-19/case-numbers-and-](https://www.health.gov.au/health-alerts/covid-19/case-numbers-and-statistics?language=und)
557 [statistics?language=und](https://www.health.gov.au/health-alerts/covid-19/case-numbers-and-statistics?language=und), Accessed: 2/6/23
- 558 14. G. E. Hartley *et al.*, The second COVID-19 mRNA vaccine dose enhances the capacity
559 of Spike-specific memory B cells to bind Omicron BA.2. *Allergy* **78**, 855-858 (2023).
- 560 15. R. R. Goel *et al.*, Distinct antibody and memory B cell responses in SARS-CoV-2 naïve
561 and recovered individuals following mRNA vaccination. *Sci Immunol* **6**, (2021).
- 562 16. W. Kim *et al.*, Germinal centre-driven maturation of B cell response to mRNA
563 vaccination. *Nature* **604**, 141-145 (2022).
- 564 17. J. S. Turner *et al.*, SARS-CoV-2 mRNA vaccines induce persistent human germinal
565 centre responses. *Nature* **596**, 109-113 (2021).

- 566 18. A. Cho *et al.*, Anti-SARS-CoV-2 receptor-binding domain antibody evolution after
567 mRNA vaccination. *Nature* **600**, 517-522 (2021).
- 568 19. P. A. Mudd *et al.*, SARS-CoV-2 mRNA vaccination elicits a robust and persistent T
569 follicular helper cell response in humans. *Cell* **185**, 603-613.e615 (2022).
- 570 20. Z. Zhang *et al.*, Humoral and cellular immune memory to four COVID-19 vaccines. *Cell*
571 **185**, 2434-2451.e2417 (2022).
- 572 21. A. Cho *et al.*, Antibody evolution to SARS-CoV-2 after single-dose Ad26.COV2.S
573 vaccine in humans. *J Exp Med* **219**, (2022).
- 574 22. R. R. Goel *et al.*, Efficient recall of Omicron-reactive B cell memory after a third dose of
575 SARS-CoV-2 mRNA vaccine. *Cell* **185**, 1875-1887.e1878 (2022).
- 576 23. W. F. Garcia-Beltran *et al.*, mRNA-based COVID-19 vaccine boosters induce
577 neutralizing immunity against SARS-CoV-2 Omicron variant. *Cell* **185**, 457-466.e454
578 (2022).
- 579 24. C. H. GeurtsvanKessel *et al.*, Divergent SARS-CoV-2 Omicron-reactive T and B cell
580 responses in COVID-19 vaccine recipients. *Sci Immunol* **7**, eabo2202 (2022).
- 581 25. A. Haveri *et al.*, Neutralizing antibodies to SARS-CoV-2 Omicron variant after third
582 mRNA vaccination in health care workers and elderly subjects. *Eur J Immunol* **52**, 816-
583 824 (2022).
- 584 26. P. Irrgang *et al.*, Class switch toward noninflammatory, spike-specific IgG4 antibodies
585 after repeated SARS-CoV-2 mRNA vaccination. *Sci Immunol* **8**, eade2798 (2023).
- 586 27. B. G. de Jong *et al.*, Human IgG2- and IgG4-expressing memory B cells display
587 enhanced molecular and phenotypic signs of maturity and accumulate with age. *Immunol*
588 *Cell Biol* **95**, 744-752 (2017).
- 589 28. G. E. Hartley *et al.*, Influenza-specific IgG1(+) memory B-cell numbers increase upon
590 booster vaccination in healthy adults but not in patients with predominantly antibody
591 deficiency. *Clin Transl Immunology* **9**, e1199 (2020).
- 592 29. E. S. J. Edwards *et al.*, Predominantly Antibody-Deficient Patients With Non-infectious
593 Complications Have Reduced Naive B, Treg, Th17, and Tfh17 Cells. *Front Immunol* **10**,
594 2593 (2019).
- 595 30. G. E. Hartley *et al.*, Rapid generation of durable B cell memory to SARS-CoV-2 spike
596 and nucleocapsid proteins in COVID-19 and convalescence. *Sci Immunol* **5**, (2020).
- 597 31. T. Kalina *et al.*, EuroFlow standardization of flow cytometer instrument settings and
598 immunophenotyping protocols. *Leukemia* **26**, 1986-2010 (2012).
- 599 32. B. Jennifer *et al.*, Transferrin receptor 1 is a cellular receptor for human heme-albumin.
600 *Commun Biol* **3**, 621 (2020).
- 601 33. S. Ni, Y. Yuan, Y. Kuang, X. Li, Iron Metabolism and Immune Regulation. *Front*
602 *Immunol* **13**, 816282 (2022).
- 603 34. A. H. Ellebedy *et al.*, Defining antigen-specific plasmablast and memory B cell subsets
604 in human blood after viral infection or vaccination. *Nat Immunol* **17**, 1226-1234 (2016).
- 605 35. S. F. Andrews *et al.*, Activation Dynamics and Immunoglobulin Evolution of Pre-
606 existing and Newly Generated Human Memory B cell Responses to Influenza
607 Hemagglutinin. *Immunity* **51**, 398-410.e395 (2019).

- 608 36. M. A. Berkowska *et al.*, Human memory B cells originate from three distinct germinal
609 center-dependent and -independent maturation pathways. *Blood* **118**, 2150-2158 (2011).
- 610 37. M. A. Berkowska *et al.*, Circulating Human CD27-IgA+ Memory B Cells Recognize
611 Bacteria with Polyreactive Igs. *J Immunol* **195**, 1417-1426 (2015).
- 612 38. J. S. Buhre *et al.*, mRNA vaccines against SARS-CoV-2 induce comparably low long-
613 term IgG Fc galactosylation and sialylation levels but increasing long-term IgG4
614 responses compared to an adenovirus-based vaccine. *Front Immunol* **13**, 1020844
615 (2022).
- 616 39. D. R. Feikin *et al.*, Duration of effectiveness of vaccines against SARS-CoV-2 infection
617 and COVID-19 disease: results of a systematic review and meta-regression. *Lancet* **399**,
618 924-944 (2022).
- 619 40. C. Menni *et al.*, COVID-19 vaccine waning and effectiveness and side-effects of
620 boosters: a prospective community study from the ZOE COVID Study. *Lancet Infect Dis*
621 **22**, 1002-1010 (2022).
- 622 41. I. Y. Addo, F. A. Dadzie, S. R. Okeke, C. Boadi, E. F. Boadu, Duration of immunity
623 following full vaccination against SARS-CoV-2: a systematic review. *Arch Public*
624 *Health* **80**, 200 (2022).
- 625 42. O. Dadras *et al.*, COVID-19 Vaccines' Protection Over Time and the Need for Booster
626 Doses; a Systematic Review. *Arch Acad Emerg Med* **10**, e53 (2022).
- 627 43. F. Muecksch *et al.*, Increased memory B cell potency and breadth after a SARS-CoV-2
628 mRNA boost. *Nature* **607**, 128-134 (2022).
- 629 44. H. Gruell *et al.*, mRNA booster immunization elicits potent neutralizing serum activity
630 against the SARS-CoV-2 Omicron variant. *Nat Med* **28**, 477-480 (2022).
- 631 45. A. K. Hvidt *et al.*, Comparison of vaccine-induced antibody neutralization against
632 SARS-CoV-2 variants of concern following primary and booster doses of COVID-19
633 vaccines. *Front Med (Lausanne)* **9**, 994160 (2022).
- 634 46. C. I. Kaku *et al.*, Broad anti-SARS-CoV-2 antibody immunity induced by heterologous
635 ChAdOx1/mRNA-1273 vaccination. *Science* **375**, 1041-1047 (2022).
- 636 47. J. Quandt *et al.*, Omicron BA.1 breakthrough infection drives cross-variant neutralization
637 and memory B cell formation against conserved epitopes. *Sci Immunol* **7**, eabq2427
638 (2022).
- 639 48. Y. Zurbuchen *et al.*, Human memory B cells show plasticity and adopt multiple fates
640 upon recall response to SARS-CoV-2. *Nat Immunol* **24**, 955-965 (2023).
- 641 49. D. Lau *et al.*, Low CD21 expression defines a population of recent germinal center
642 graduates primed for plasma cell differentiation. *Sci Immunol* **2**, (2017).
- 643 50. S. A. Jenks *et al.*, Distinct Effector B Cells Induced by Unregulated Toll-like Receptor 7
644 Contribute to Pathogenic Responses in Systemic Lupus Erythematosus. *Immunity* **49**,
645 725-739.e726 (2018).
- 646 51. H. C. Matz, K. M. McIntire, A. H. Ellebedy, 'Persistent germinal center responses: slow-
647 growing trees bear the best fruits'. *Curr Opin Immunol* **83**, 102332 (2023).
- 648 52. B. J. Laidlaw, A. H. Ellebedy, The germinal centre B cell response to SARS-CoV-2. *Nat*
649 *Rev Immunol* **22**, 7-18 (2022).

- 650 53. V. Irani *et al.*, Molecular properties of human IgG subclasses and their implications for
651 designing therapeutic monoclonal antibodies against infectious diseases. *Mol Immunol*
652 **67**, 171-182 (2015).
- 653 54. G. Vidarsson, G. Dekkers, T. Rispens, IgG subclasses and allotypes: from structure to
654 effector functions. *Front Immunol* **5**, 520 (2014).
- 655 55. A. W. Chung *et al.*, Polyfunctional Fc-effector profiles mediated by IgG subclass
656 selection distinguish RV144 and VAX003 vaccines. *Sci Transl Med* **6**, 228ra238 (2014).
- 657 56. C. Dobaño *et al.*, Age-dependent IgG subclass responses to Plasmodium falciparum
658 EBA-175 are differentially associated with incidence of malaria in Mozambican
659 children. *Clin Vaccine Immunol* **19**, 157-166 (2012).
- 660 57. L. H. Hendriks *et al.*, Different IgG-subclass distributions after whole-cell and acellular
661 pertussis infant primary vaccinations in healthy and pertussis infected children. *Vaccine*
662 **29**, 6874-6880 (2011).
- 663 58. J. J. Heeringa *et al.*, Induction of IgG(2) and IgG(4) B-cell memory following sublingual
664 immunotherapy for ryegrass pollen allergy. *Allergy* **75**, 1121-1132 (2020).
- 665 59. C. I. McKenzie *et al.*, RNA sequencing of single allergen-specific memory B cells after
666 grass pollen immunotherapy: Two unique cell fates and CD29 as a biomarker for
667 treatment effect. *Allergy* **78**, 822-835 (2023).
- 668 60. S. Pillai, Is it bad, is it good, or is IgG4 just misunderstood? *Sci Immunol* **8**, eadg7327
669 (2023).
- 670 61. R. Munemura *et al.*, Distinct disease-specific Tfh cell populations in 2 different fibrotic
671 diseases: IgG(4)-related disease and Kimura disease. *J Allergy Clin Immunol* **150**, 440-
672 455.e417 (2022).
- 673 62. S. Terreri *et al.*, Persistent B cell memory after SARS-CoV-2 vaccination is functional
674 during breakthrough infections. *Cell Host Microbe* **30**, 400-408.e404 (2022).
- 675 63. T. A. Bates *et al.*, Vaccination before or after SARS-CoV-2 infection leads to robust
676 humoral response and antibodies that effectively neutralize variants. *Sci Immunol* **7**,
677 eabn8014 (2022).
- 678 64. M. Akkaya, K. Kwak, S. K. Pierce, B cell memory: building two walls of protection
679 against pathogens. *Nat Rev Immunol* **20**, 229-238 (2020).
- 680 65. R. R. Goel *et al.*, mRNA vaccines induce durable immune memory to SARS-CoV-2 and
681 variants of concern. *Science* **374**, abm0829 (2021).

682 **FIGURE LEGENDS (n=5)**



683

684 **Figure 1: Third dose booster significantly increases WH1 RBD-specific plasma IgG and**

685 **Bmem.** (A) Schematic of patient cohorts, vaccination schedules and sampling timepoints.

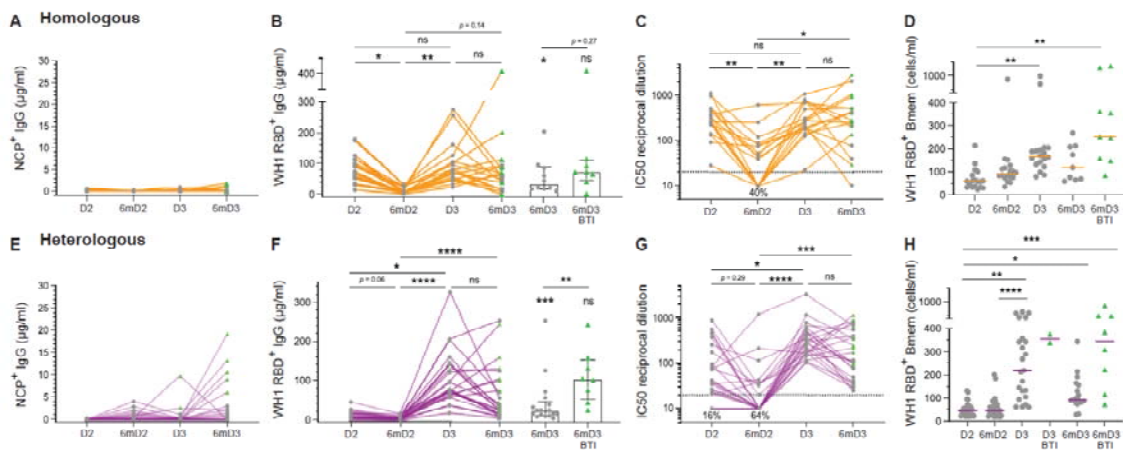
686 Details in **Supplementary Tables 1-3.** (B) Ancestral (WH1) RBD-specific plasma IgG levels

687 and (C) neutralizing antibodies (NAb) in individuals who received a primary BNT162b2

688 (BNT) or ChAdOx1 (ChAd) vaccination followed by an mRNA third dose booster. (D)

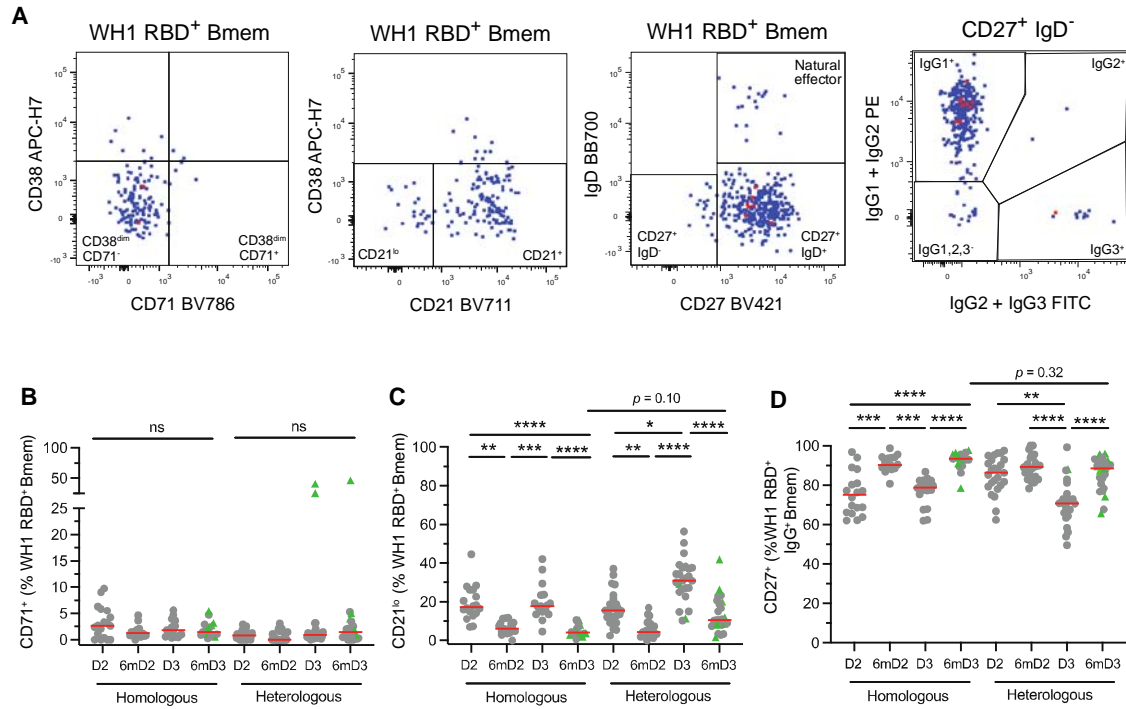
689 Detection of ancestral RBD-specific Bmem using double discrimination with recombinant
 690 WH1 RBD tetramers. (E) WH1 RBD-specific Bmem numbers following 2 doses of BNT or
 691 ChAd and after mRNA third dose booster. Green triangles represent individuals who had a
 692 confirmed breakthrough infection (BTI) prior to sampling (**Supplementary Tables 1 and 2**).
 693 Red lines in panels B, C and E represent median values. Kruskal-Wallis test with Dunn's
 694 multiple comparisons test. ** $p < 0.01$, **** $p < 0.0001$.

695



696

697 **Figure 2: Ancestral (WH1) RBD-specific plasma IgG and Bmem dynamics following**
 698 **homologous or heterologous vaccination.** (A) NCP-specific, (B) WH1 RBD-specific, (C)
 699 Neutralizing antibody (NAb) levels and (D) WH1 RBD-specific Bmem numbers following
 700 homologous vaccination (n = 18). (E) NCP-specific, (F) WH1 RBD-specific, (G) NAb levels
 701 and (H) WH1 RBD-specific Bmem numbers following heterologous vaccination (n = 25).
 702 Green triangles represent individuals who had a confirmed breakthrough infection (BTI) prior
 703 to sampling (**Supplementary Tables 1 and 2**). Red lines in panels D and H represent median
 704 values. Significance stars above bars in B and F depict comparisons to the 1-month post-dose
 705 3 measurements. Kruskal-Wallis test with Dunn's multiple comparisons test. * $p < 0.05$, ** p
 706 < 0.01 , **** $p < 0.001$, **** $p < 0.0001$



707

708 **Figure 3: mRNA third dose generates a transient population of recently activated**

709 **ancestral (WH1) RBD-specific Bmem.** (A) Definitions of CD38^{dim}CD71⁺, CD21^{lo} and

710 CD27⁺IgG⁺ WH1 RBD-specific Bmem. Proportions of WH1 RBD-specific (B)

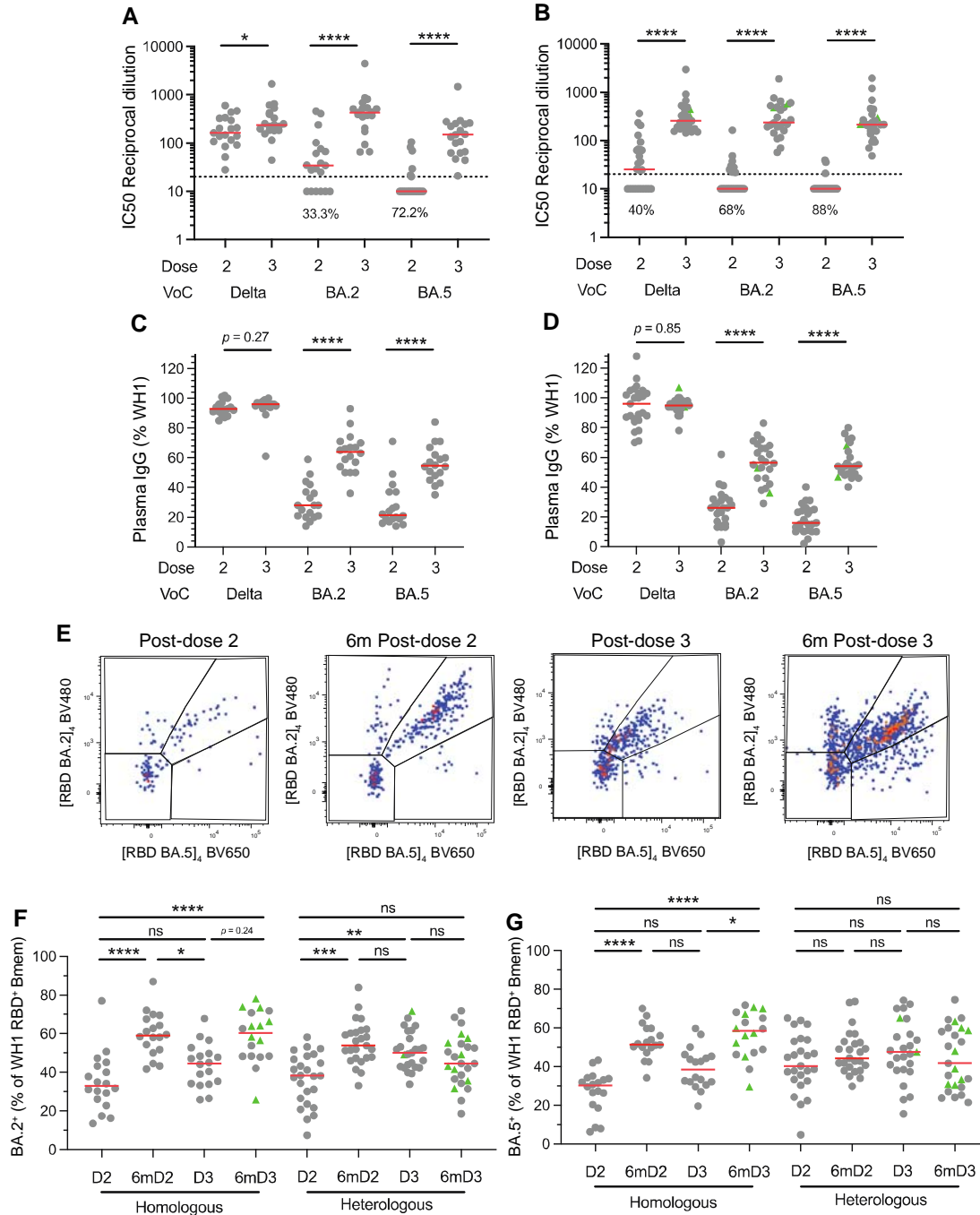
711 CD38^{dim}CD71⁺ Bmem (C) CD21^{lo} Bmem (D) and CD27⁺IgG⁺ Bmem in the homologous (n =

712 18) and heterologous (n = 25) vaccination groups. Green triangles represent individuals who

713 had a confirmed breakthrough infection (BTI) prior to sampling (Supplementary Tables 1

714 and 2). Red lines in panels B-D represent median values. Kruskal-Wallis test with Dunn's

715 multiple comparisons test. * $p < 0.05$, ** $p < 0.01$, *** $p < 0.001$, **** $p < 0.0001$.



726

727 **Figure 5: Third dose booster vaccination increases recognition of Omicron BA.2 and**
 728 **BA.5 variants.** Neutralization of Delta and Omicron BA.2 and BA.5 variants in the (A)
 729 homologous and (B) heterologous vaccination groups. Recognition of ancestral (WH1) RBD-
 730 specific plasma IgG to Delta and Omicron BA.2 and BA.5 variants in the (C) homologous
 731 and (D) heterologous vaccination groups. (E) Identification of WH1 RBD-specific Bmem

732 that also bind Omicron BA.2 and BA.5 variants. Capacity of WH1 RBD-specific Bmem to
733 recognise Omicron (F) BA.2 and (G) BA.5 in the following homologous (n = 18) and
734 heterologous vaccination groups (n = 25). Green triangles represent individuals who had a
735 confirmed breakthrough infection (BTI) prior to sampling (**Supplementary Tables 1 and 2**).
736 Red lines in panels C and D represent median values. Wilcoxon signed rank test with
737 Bonferroni correction for multiple comparisons for panels A-D. Kruskal-Wallis test with
738 Dunn's multiple comparisons test for F and G. * $p < 0.05$, ** $p < 0.01$, **** $p < 0.0001$.